

Certain Characteristics of Composite Polytetrafluoroethylene-Oxide Coatings on Aluminum Alloy

V. S. Rudnev^{a, b}, A. A. Vaganov-Vil'kins^a, A. K. Tsvetnikov^a, P. M. Nedozorov^a,
T. P. Yarovaya^a, V. G. Kuryavy^a, E. E. Dmitrieva^a, and E. A. Kirichenko^c

^a Institute of Chemistry, Far-Eastern Branch, Russian Academy of Sciences,
159 Prosp. 100-letiya Vladivostoka, Vladivostok, 690022 Russia

^b Far Eastern Federal University, 8 Suhanova St., Vladivostok, 690590 Russia

^c Institute for Material Studies, Khabarovsk Scientific Center, Far-Eastern Branch,
Russian Academy of Sciences, 153 Tikhookeanskaya St., Khabarovsk, 680042 Russia

e-mail: rudnevvs@ich.dvo.ru

Received July 2, 2014

Abstract—We present the results of an investigation of the distribution of elements according to cross-section morphology, adhesion, and anticorrosive properties of PTFE-oxide layers formed by plasma-electrolytic oxidation in an $\text{Na}_2\text{SiO}_3 + \text{NaOH}$ electrolyte with dispersive particles of PTFE stabilized by siloxane acrylate emulsion. Coatings have a structure uncharacteristic of PEO layers. The main coating mass of thickness of up to 80 μm is composed of polytetrafluoroethylene and decomposition products of PTFE particles, as well as of the emulsion. The transition layer between the metal and polymer coating has a thickness of $\sim 10 \mu\text{m}$ and contains oxides of aluminum and silicon. Sample weight loss after ultrasonic treatment in water is $\sim 1\%$, which indicates a satisfactory adhesion of the coating to the metal and the cohesion between coating fragments. The coatings have a complex surface with pores several tens of microns in size. After annealing in air at 200°C, pores are filled with polymer, which is accompanied by a significant improvement in the coating's anticorrosive properties. As a result of annealing in air at 400°C, the polymer coating sublimates and the transition layer with a thickness of $\sim 10\text{--}15 \mu\text{m}$ remains.

DOI: 10.1134/S2070205115010128

INTRODUCTION

Composite layers that contain organic and inorganic phases—for example, polymer-oxide or graphite-oxide coatings on metals—applied by different methods are attracting attention from various points of view [1–13]. These coatings may be antifriction, with a low coefficient of friction [1–3], protective with improved microhardness and wear and corrosion resistance [1, 3–9], hydrophilic [11], hydrophobic [12], superhydrophilic or superhydrophobic [13], and preventative of salt deposition at elevated temperatures in mineralized water (salt deposition in heat exchangers) [12].

In recent years, to form coatings on metals, including composite coatings of varying compositions and functions, electrochemical oxidation and deposition in electric spark or microarc discharge conditions on the metal/electrolyte boundary is widely used [14–16]. In the literature, this method is called plasma electrolytic oxidation (PEO), microarc or microplasma oxidation (MAO), or anodic spark electrolysis. In this text, we will use the term “plasma electrolytic oxidation.” The process is conducted at anodic, mixed anodic–cathodic, or cathodic polarization. An important treatment characteristic is the formation on

the surface of metal or alloy of not only an oxide layer from substrate components, but also the implantation into the growing oxide of electrolyte components with their various thermal phases, as well as the formation of appropriate oxides and the participation in high-temperature interactions in zones adjacent to the electric spark or arc discharge channels [14–16]. From a technological point of view, we can also consider the following to be positive characteristics of the method: the formation of coatings is performed at solution temperature of no higher than 100°C, that the method permits treatment of high-profile products, there is good adhesion between the metallic base and the applied coating, and there is relative simplicity of the experimental setup and a small treatment time (no more than a few hours).

In many cases, composite coatings are formed in several stages using various methods, including PEO. For example, in previous work [7], to form a composite corrosion resistant layer on a magnesium alloy, it was initially oxidized through PEO to create a porous oxide coating. Afterward, the pores were filled with a corrosion inhibitor, with subsequent pore sealing using the sol–gel method. In another example [12], a layer of PTFE dispersed particles with a size of no greater than 1 μm was applied using a tribological method

(mechanical rubbing) onto a PEO coating, which gave the surface hydrophobic properties and significantly increased the protective properties of the resultant composite coating [12, 16]. The authors of these works believe that the tribological application of PTFE particles leads to the sealing of pores and cracks by “plugs” composed of PTFE particles. The conclusion is supported by the improved protective properties resulting from annealing of resultant hybrid coatings at temperatures above PTFE T_g (in the neighborhood of 100–260°C for various compositions) [12–16]. To improve the corrosion resistance of coatings on a magnesium alloy after PEO in electrolytes containing TiO_2 , ZrO_2 , and Al_2O_3 nanoparticles, silanes (octyltrimethoxysilane and 1,2-bis triethoxysilylletane) were additionally deposited on the coating for the purpose of sealing pores and cracks [5].

There is little doubt that the formation of composite coatings in one step is more acceptable than multi-stage treatment. Developments of single-stage approaches using PEO methods have attracted much attention [1, 2, 6, 17–21]. It has been shown in several works that the introduction of dispersed graphite particles into electrolyte not only reduces the friction coefficient and, as a result, wear resistance, but also increases the corrosion resistance of PEO coatings formed on valve metals [1, 2]. The influence of the introduction into an electrolyte of dispersed claylike particles with a relatively low melting temperature on the formation process and the structure of PEO coatings on a magnesium alloy has been investigated [6]. It was shown that, as a result of the baking of the claylike particles with the oxide layer, the microstructure of the latter changes significantly.

It is important to develop approaches for the application of protective coatings onto the surface of iron, low-carbon steel, and stainless steel products [17–21]. One of the investigated PEO methods—conductance of high voltages through the electrode—leads to liberal production of gases in the near-electrode region, heating of the metal, boiling of electrolyte at its surface, formation around the electrode of a gaseous layer, and electrical breakdown. During this, the coating is formed from electrolyte components. Mass transfer from the electrolyte is performed via an electrical spark or arc discharges. It has been shown that the addition of ethylene powder PENDING 273-83 into the hydrous electrolyte $NaAlO_2 + NaOH$ sharply reduces the initial current density during the potentiodynamic formation of PEO coatings on low-carbon steel due to the screening of portions of the electrode's surface by the polymer [20]. At low formation times coatings primarily consist from polymer particles reinforced by oxide-hydroxide aluminum compounds. For example, formation for 1 min results in coatings with a thickness of 20 μm and composition of 79.9 at % C, 2.9 at % Al, and 17.8 at % O according to microprobe analysis data. With increasing treatment time, the polymer (or carbon) content in the coating decreases.

Thus, after 30 min, the composition of the coating of thickness 104 μm is 25.6 at % C, 16.5 at % Al, and 57.4 at % O.

One of the issues in using hydrous electrolytes with dispersed organic particles, for example polymer or graphite during PEO is their stabilization in solution. In our previous works [22–25], we have suggested using emulsion–suspension electrolytes for stabilization of dispersed PTFE particles with a size of around 1 μm or graphite particles with a size of around 70 μm in hydrous electrolyte. In these cases, the suspension of dispersed PTFE or graphite was thoroughly mixed with a necessary volume of KE 13-36 siloxane-acrylate emulsion produced by Astrokhim (Russia). In this process, we believe, emulsion micelles are adsorbed onto dispersed particles (encasing them), improving their wetting properties and giving their surfaced a negative charge. When introducing the mixture into a hydrous base electrolyte containing $Na_2SiO_3 + NaOH$, a stable hydrous suspension is formed that does not separate for months. PEO was performed in this suspension. Schematics of the structure of the dispersed particle in electrolyte and of the coating formation are presented in Fig. 1.

When using electrolytes with dispersed PTFE particles, the formation, thickness, appearance, surface morphology, surface elemental and phase composition, and wetting and mechanical wear under stress characteristics depended on the amount of PTFE powder introduced into the electrolyte (electrolytes contained 100 mL/L emulsion containing 10–60 g/L PTFE particles) [22–25]. All the coatings under investigation contained a significant amount of carbon. For example, in an electrolyte containing 40 g/L PTFE particles, coatings with a thickness of ~40 μm formed over 20 min contained, according to microprobe analysis (analysis depth 2–5 μm), 69.9 at % C, 24.5 at % O, 1 at % F, 1.5 at % Al, and 2.9 at % Si. When the powder concentration was 60 g/L, coatings with a thickness of ~80 μm were formed with composition 58.1 at % C, 12 at % O, 29.2 at % F, 0 at % Al, and 0.6 at % Si. Thus, the coating surface region (thickness of 2–5 μm) consists primarily of electrolyte components—specifically, PTFE and products of decomposition of PTFE and emulsion by electric discharges. At PTFE particle concentrations of greater than 30 g/L, peaks are present in X-ray diffraction patterns that correspond to PTFE. Additionally, regions of light and dark coloring are present on the surface, as can be seen in Fig. 1b. The presence of PTFE and the products of its decomposition in coatings significantly (by several orders of magnitude) increases the mechanical wear time of coatings under stress and confers hydrophobic properties to the surface. In general, the data on the composition of carbon, aluminum, and oxygen in a coating surface correlate with the composition of the surface region of coatings produced in earlier works [20, 21] on low-carbon steel in an electrolyte containing dispersed polyethylene particles.

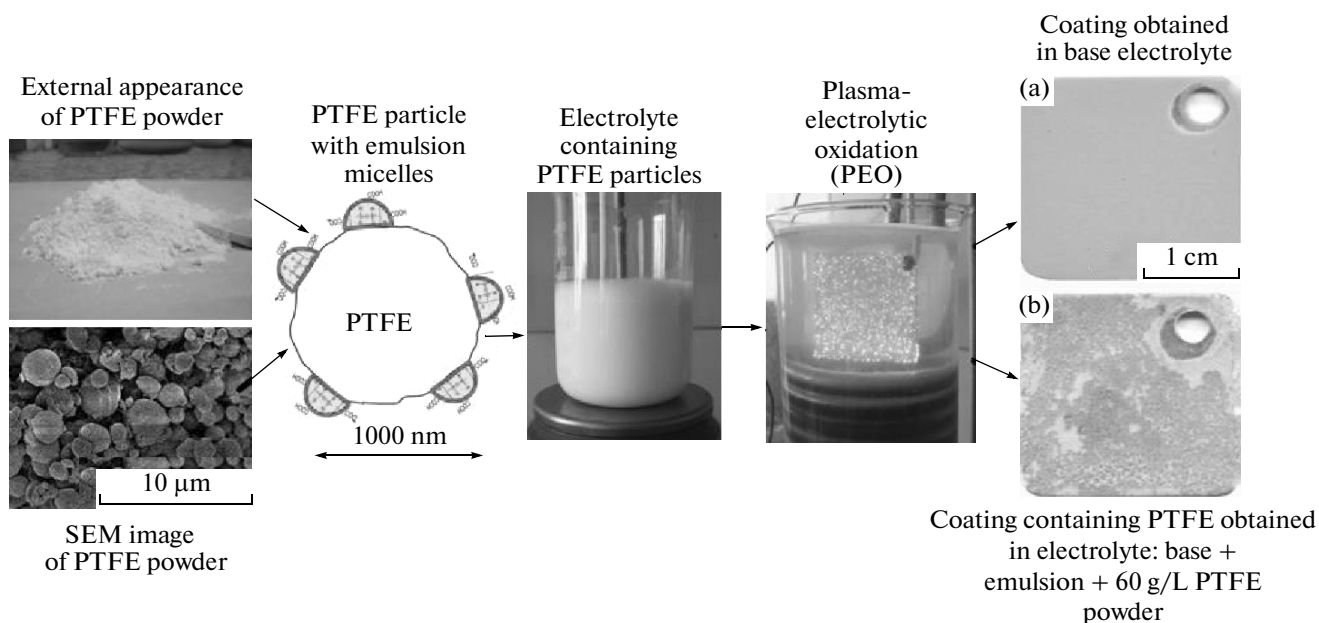


Fig. 1. Preparation scheme of suspension-emulsion electrolyte with PTFE particles and the formation of composite coatings containing PTFE and its decomposition products.

We learned later that the principle of using an acrylate emulsion to stabilize PTFE particles in a PEO electrolyte had been set out and proven in another article [26]. The size of the PTFE particles used is not reported in this article. The base electrolyte, as in our case, contained $\text{Na}_2\text{SiO}_3 + \text{NaOH}$. A bipolar pulsed current of a constant effective density of 4.5 A/dm^2 was used to form coatings on aluminum alloy. The use of electrolyte with PTFE particles led to a change in the surface morphology and pore closing. According to *X*-ray photoelectron spectroscopy, an *F*1s peak with a bond energy of 690 eV is present in the coating composition that corresponds to the CF_2 group; i.e., the coating contains PTFE. According to potentiodynamic measurements, in 3% NaCl, the base coating and PTFE coating have approximately equal corrosion potentials ($-1.60 \pm 0.007 \text{ V}$ without and $-1.56 \pm 0.004 \text{ V}$ with PTFE). However, for PTFE coatings, the corrosion current was an order of magnitude lower than for coatings formed in the base electrolyte ($-2.508 \pm 0.04 \times 10^{-6} \text{ A/dm}^2$ with and $2.141 \pm 0.03 \times 10^{-7} \text{ A/dm}^2$ without PTFE). The measured coefficient of friction for the base coating was ~ 0.55 , and it was ~ 0.15 for coating containing PTFE.

In this manner, according to our research [22–25] and literature data [26], the use of suspension–emulsion electrolytes with PTFE particles permits the implantation of PTFE into coatings. This gives coatings hydrophobic, antifriction, and wear-resistant properties and, as to [26], improves the protective properties of coatings in chlorine-containing environments. This approach is viable for the production of composite PTFE-oxide layers on the surface of valve

metals. However, many characteristics of coatings containing PTFE and its decomposition products have been insufficiently investigated. For example, their coating growth kinetics, their cross-sectional structure, their protective characteristics, and the influence of temperature on coating properties and composition. This work is dedicated to addressing these issues.

MATERIALS AND METHODS

Composite layers were formed on samples of AMg5 aluminum with a size of $20 \times 20 \times 0.5 \text{ mm}$. Prior sample preparation included mechanical with subsequent chemical polishing in an acidic mixture of $\text{H}_3\text{PO}_4 : \text{H}_2\text{SO}_4 : \text{HNO}_3 = 4 : 2 : 1$ at $90\text{--}100^\circ\text{C}$.

For preparation of the base electrolyte, distilled water and “hc” brand commercial reagents were used: $10.6 \text{ g/L Na}_2\text{SiO}_3 \cdot 5\text{H}_2\text{O}$ and 2 g/L NaOH . KE 13-36 commercial siloxane-acrylate emulsion produced by Astrokhim (Russia) was used as an emulgator. Forum (Russia) polydispersed PTFE powder with a majority fraction particle size of $\sim 1 \mu\text{m}$ was used.

The working electrolyte was prepared in two stages. First, 100 mL of siloxane-acrylate emulsion was mixed with the necessary amount of PTFE powder. The mixture was thoroughly mixed, providing full wetting of PTFE particles by the siloxane-acrylate emulsion. The resulting mixture was combined with a base electrolyte. The final product was a complex emulsion-suspension with a dispersed phase of hard PTFE particles “encased” by the siloxane-acrylate emulsion, giving the particles a negative surface charge and pre-

venting their agglomeration. The electrolyte is stable for at least over a month of observation, and separation of the emulsion–suspension was practically unobserved.

Electrochemical treatment of aluminum samples was performed in a temperature-resistant glass beaker filled with electrolyte. The counterelectrode was a hollow spiral of nickel alloy. Cold running water was passed through the spiral to cool the mixture. The mixture temperature during treatment did not exceed 30°C. The current source was a TER-4/460N computer-controlled thyristor device (Russia) operating in a unipolar regime. The electrolyte was mixed using a mechanical stirrer. Anodic coatings were acquired over a duration of 20 min at an effective current density of 0.05 A/cm². Coated samples were washed with distilled water and dried in air.

Film thickness was measured using a VT-201 (Russia) thickness gauge. Sample annealing at set temperatures was performed in a muffle furnace in air for 1 h.

Elemental composition and surface layer micrographs were acquired using a JXA-8100 Electron Probe Microanalyzer (Japan). The amount of a given element was determined as the mean of five measurements taken in various regions on the film during scanning of film sections of size 300 × 200 μm.

High-resolution micrographs were acquired using a Scanning Electron Microscope HITACHI S-5500 (Japan). An energy dispersive X-ray analysis module from Thermo Scientific (United States) was used to determine the elemental composition of both film sections and individual points of diameter up to 50 nm with an analysis depth of ~1 μm.

Phase composition was determined using a D8 ADVANCE X-ray diffractometer with sample rotation around CuK_α-rays. EVA search software with the PDF-2 database was used for X-ray diffraction data analysis.

The contact angle between the surface/distilled water interface was measured using a “sitting drop” method. The coated sample was placed on an optical table with the possibility of adjustment of the sample position. A pipette was used to apply a drop of distilled water onto the sample. A Canon PowerShot G6 digital camera was used to photograph the drop that had been applied onto the coating surface. The photo image was subsequently transferred to a personal computer, and image editing software was used to measure the contact angle. Four drops in total were applied to every sample, contact angles were measured from various sides of the drop’s profile, and measurement results were averaged.

Coating adhesion was evaluated based on the change in sample mass after ultrasonic treatment in water [27, 28]. The emitter power was 140 W, the water temperature was 25°C, and the treatment time was 20 min. The sample was initially weighed and then placed approximately 3 cm from the emitter. The cell

had an inbuilt reflector that allowed the treatment of both sides of the sample simultaneously. After ultrasonic treatment, samples were dried at 90°C in air and subsequently weighed again. Measurements were performed on series of three samples, and measurement results were averaged.

The pitting formation time during initiation of the process by potential difference ($U = 1$ and 8 V) applied to the boundary between a coating and 3% hydrous NaCl solution was used to determine coating corrosion resistance (shown in Fig. 2). A syringe with a metal needle was filled with 3% NaCl solution. The needle was connected with the minus end of the current source. The plus of the current source was connected to the bare sample metal across an ammeter. Using a screw, a drop of 3% NaCl solution was squeezed out onto the coating. A stopwatch was used to measure the interval between the drop touching the surface and the sharp increase of current through the sample.

Three-dimensional images of the surface, as well as surface roughness data, were acquired using a LEXT OLS3100 confocal laser scanning microscope (Japan).

RESULTS

Structure and Morphology of Coatings

For the formation of coatings that are homogeneous in appearance and thickness, a study of the suspension–emulsion electrolyte with PTFE particles is required. For example, using a freshly-prepared electrolyte containing 10 g/L of PTFE powder on the first sample treated for 20 min, a relatively smooth, homogeneous, brown-tinted coating with a thickness of 9 ± 2 μm is formed, as is shown in Fig. 1a. In subsequent samples, in the same treatment period, coatings are formed containing white and dark regions similar to the one shown in Fig. 1b. The coating thickness increases. In these cases, for 2 min after treatment begins, the sample surface appears light (covered by a white layer). Subsequently, dark (brown-tinted) regions begin to grow on the white-colored coating. By increasing the treatment time, the entire surface can be made “dark.” However, this transition takes a prolonged period of time and, depending on the concentration of PTFE powder in the electrolyte and sample size, may take up to 50 min or more.

Light and dark regions differ in surface morphology, as is shown in Figs. 3c and 3d. Light regions have a notably less complex surface and smaller pore size. The confocal laser microscope data shown in Fig. 3e confirm the scanning electron microscopy findings.

According to confocal laser microscopy, dark regions sit above light regions (Fig. 3e). The difference in height between the regions for the studied coating can be up to 35 μm. We note that the average coating thickness, measured by an eddy-current thickness

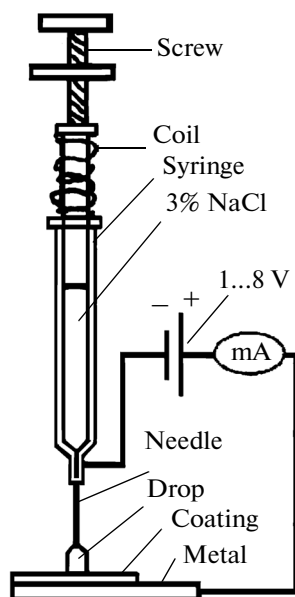


Fig. 2. Measurement scheme of pitting formation time initiated by applied potential difference from 1 to 8 V. Substrate metal has positive polarization.

gauge in this case (base electrolyte + 100 mL/L emulsion + 60 g/L PTFE powder), is $80 \pm 10 \mu\text{m}$ [23].

In Table 1, we present microprobe analysis data on the elemental composition of dark and light surface regions. The elemental composition was determined in every case for five randomly selected regions of a size of $300 \times 200 \mu\text{m}$, and it was then averaged. We note that, for this method, depending on the material in question, the analysis depth ranged from 2 to $5 \mu\text{m}$.

From the data in Table 1, it can be seen that the production of coatings in a base electrolyte without dispersed PTFE, the coatings, along with the oxides of metals present in the aluminum alloy (Al, Mg), contain compounds both based on the components of the base solution (Na, Si) and based on the emulsion (carbon). Additionally, according to previously acquired data, the addition of emulsion into the base electrolyte does not significantly influence the coating thickness ($8 \pm 2 \mu\text{m}$ in both cases [23]). The introduction of dispersed PTFE powder into the base electrolyte along

with the emulsion increases the thickness up to several tens of microns and fundamentally changes the surface composition, as is shown in table 1. Aluminum, magnesium, and sodium are absent in the composition of the light and dark regions. The concentration of silicon and oxygen significantly decreases. Conversely, the concentration of carbon increases sharply and fluorine can be observed in the coating composition. These facts indicate that, in these cases, the coating surface contains mostly PTFE and, as the carbon composition exceeds the stoichiometric norm for PTFE, products of decomposition by electric discharge of both dispersed PTFE particles and the emulsion. We note that, according to the literature, the temperature in electric breakdown channels can reach several thousands of degrees [14–16]. The coating regions adjacent to these channels will heat up accordingly. The heating may lead to the partial sublimation of PTFE, its softening and transition to a viscous state, and fusing of particles. A full sublimation does not occur due to the short discharge time ($\sim 10^{-3} - 10^{-5}$ s) [29] and subsequent fast cooling of heated regions due to their low thickness and heat transfer into metal and room-temperature electrolyte. The decomposition products of PTFE may be ash or other carbon-containing products and compounds, among them a short-chain polymer. According to the literature data, Forum dispersed PTFE contains components with a carbon count from C_5 to C_{70} , the majority of which are saturated and unsaturated carbon fluorides [30].

As can be seen from Table 1, The dark regions that sit on the light regions contain one-third less fluorine. Thus, they contain less PTFE and are mostly formed from carbon, as opposed to the light regions. Simultaneously, these regions are characterized by a rougher profile and by large notches in the coating mass, as shown in Fig. 3. It is evident that the dark regions are formed as a result of the activity of strong electrical discharges in these regions—for example, microarc discharges—and contain the decomposition products of PTFE and the emulsion. This conclusion correlates with the eventual covering of the entire surface by dark regions with increased coating formation duration.

Table 1. Elemental composition of coatings formed in base electrolyte + 100 mL/L emulsion with addition of 60 g/L dispersed PTFE powder

PTFE powder concentration, g/L	Elemental composition, at %						
	Al	O	Mg	Na	C	F	Si
0	12.4 ± 0.1	38.2 ± 1.1	0.8 ± 0.06	0.4 ± 0.03	44.6 ± 2.0	—	3.6 ± 0.3
60, light region	—	12.1 ± 1.1	—	—	58.1 ± 2.1	29.2 ± 1.8	0.6 ± 0.07
60, dark region	—	16.8 ± 1.2	—	—	63.6 ± 1.3	18.9 ± 1.9	0.7 ± 0.14

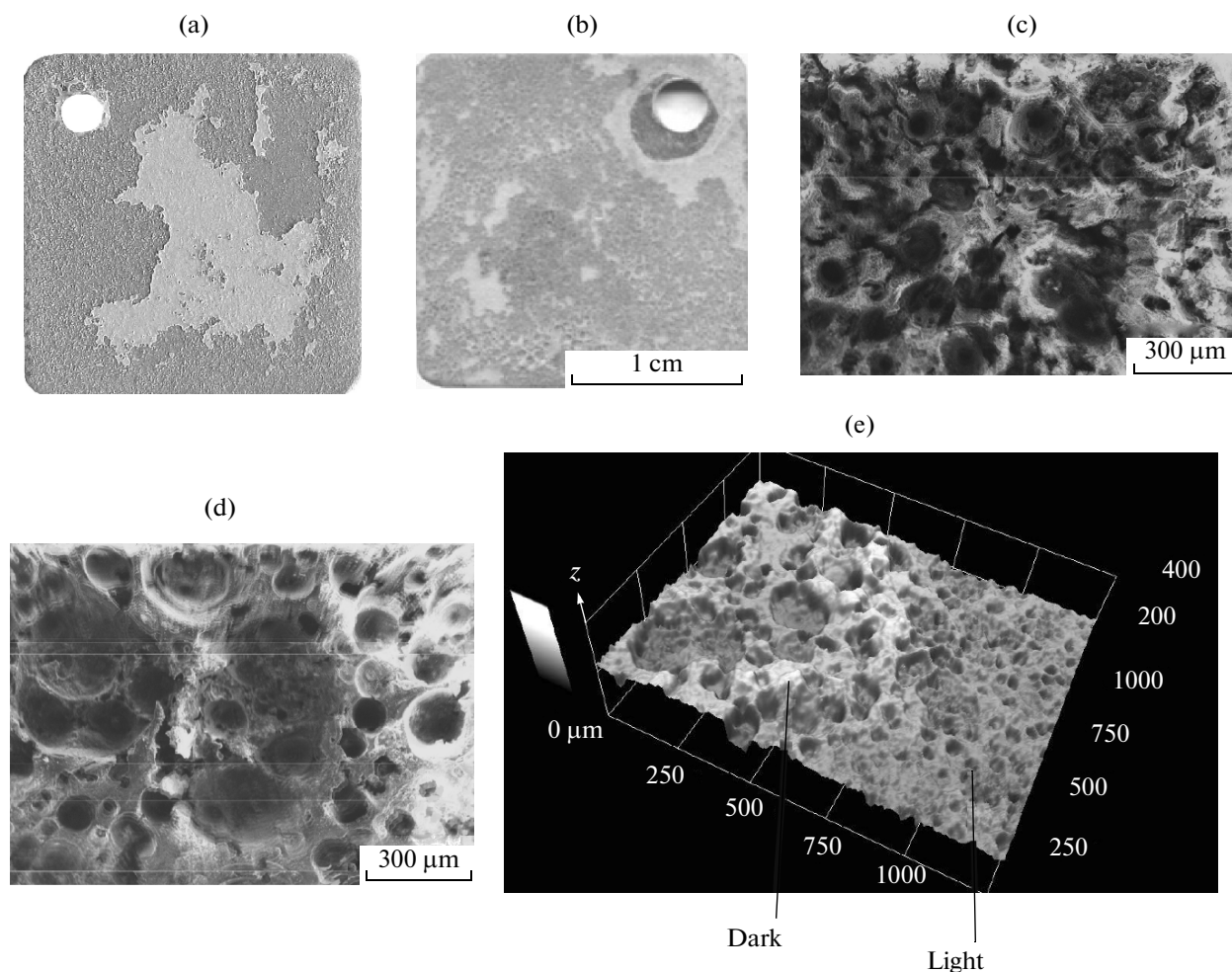


Fig. 3. Exterior appearance of coatings formed over 20 min in base electrolyte + 100 mL/L emulsion + (a) 10 or (b) 60 g/L PTFE powder. Morphology of (c) light or (d) dark regions on the coating surface formed when PTFE concentration in electrolyte is 60 g/L. (e) Height difference between light and dark surface regions.

Coating Cross-Sectional Structure

According to Table 1, the surface layer of the resulting coatings consists primarily of PTFE and high temperature products of PTFE particles and the emulsion. It is of significant interest to study the structure of resultant coatings along their cross section. As a large amount of carbon is contained within the coatings, the standard methods of section preparing involving grinding papers and carbon-containing pastes are in this case of little use due to the difficulty of interpreting findings on carbon content. Due to this, the following methods were used. In the first case, the tip of an aluminum wire was carefully milled. Afterward, a drop of superglue was applied to the tip, making sure that the glue did not touch the wire's sides and conformed as much as possible to the wire's diameter. After polymerization of the superglue drop, the wire was oxidized in an electrolyte with 60 g/L PTFE particles. Afterward, the solidified drop was removed from the wire with a sharp instrument. In Fig. 4a, a portion is

shown of the tip of the wire and the surrounding cross-sectional surface fracture. Sections for investigation with the clearest borders between tip and coating were selected using a microscope, as shown in Fig. 4b.

In the second case, a mechanical slice of the coating/alloy system was made using a well-sharpened cutting tool, as shown in Fig. 5a.

In both cases, the cross-sectional coating thickness is about 100 μm , which is similar to the value determined by the eddy current thickness gauge of $80 \pm 10 \mu\text{m}$ [23]. It is clear that the coating on the cross section is not homogeneous. In Figs. 4a and 5a, caverns and elongated white regions can be observed in the depth of the coatings. A section of coating selected for the determination of elemental variation across the thickness of a coating was constructed from regions of different coloring, as shown in Fig. 4b.

Elemental composition data relative to distance to the aluminum substrate are shown in Figs. 4c and 5b. In both cases, it is evident that the composition drops

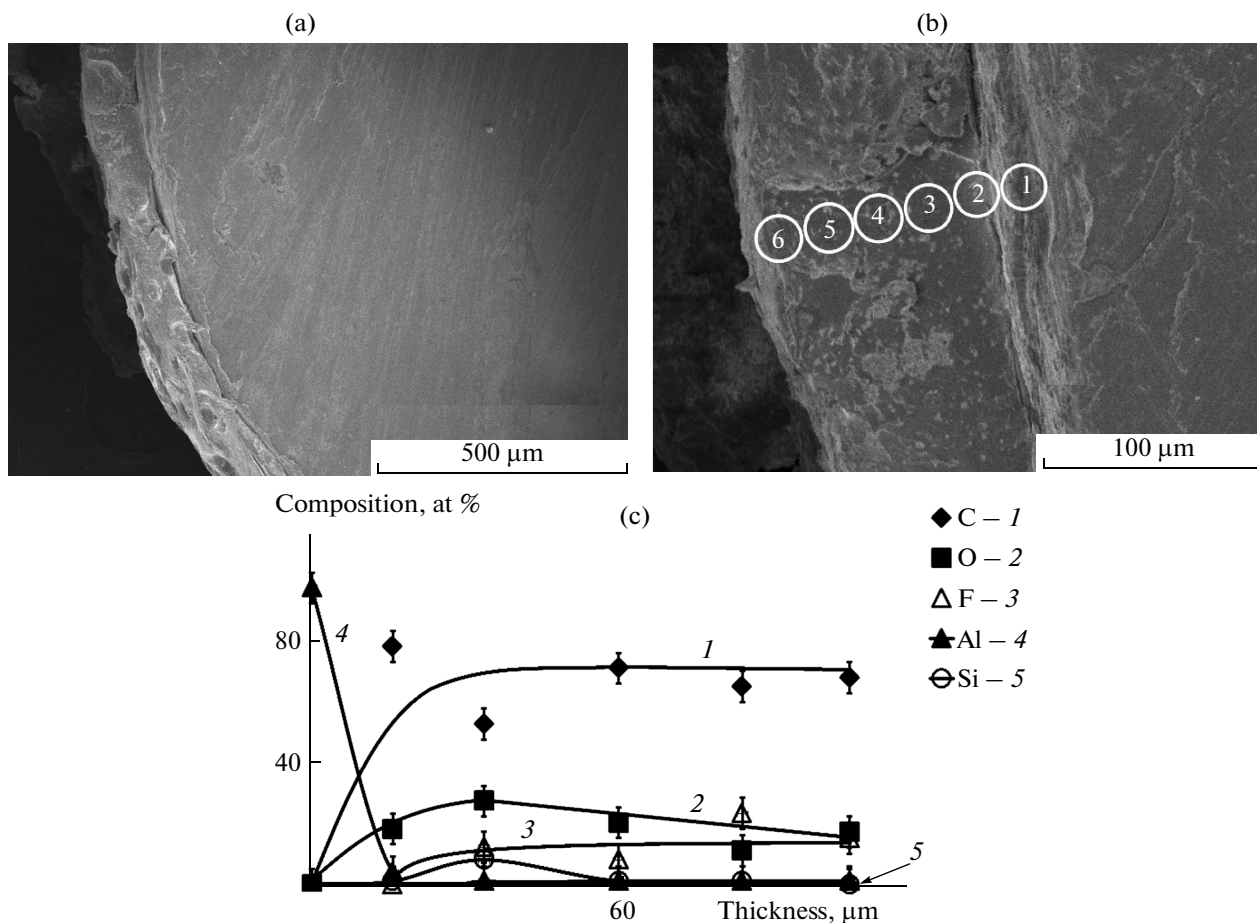


Fig. 4. Wire tip with (a) coating section, (b) selected cross-section region for investigation of surface elemental composition, and (c) elemental distribution across coating thickness.

practically to zero at 10 μm from the substrate. In this same interval, the concentration of carbon increases up to 50–70 at % and that of oxygen increases up to 20 at %. The concentration of fluorine in both cases gradually increases up to the coating/air boundary, reaching 20–25 at %. Aluminum and fluorine exist in concentrations of a few percent in the depth of the coating.

High-magnification investigation of cross sections, as shown in Fig. 6, shows that agglomerates of particles with a size of approximately 1 μm exist inside the caverns sealed within the coatings. According to energy dispersive spectroscopy, they contain 51 at % C, 45 at % F, and 4 at % O. Taking into account the probe beam's penetration depth into the main mass of the coating, it is highly likely that the dispersed particles are PTFE particles captured from the electrolyte. We note that similar agglomerates have been observed in pores at the coating surface [23].

The elemental composition of the coatings shown in Figs. 4c and 5b and determined using the energy dispersive module of the scanning electron microscope closely correlates to the elemental composition determined for the top 2–5 μm of the coating deter-

mined by microprobe analysis, as shown in Table 1. Thus, for the majority of its thickness, the composition of a coating is relatively homogeneous, being products of partial sublimation, decomposition, and melting of the emulsion and PTFE particles that have been, apparently, reinforced by aluminum and silicon oxides. In the region adjacent to an aluminum substrate of thickness of approximately 10 μm , a gradual transition occurs from aluminum to aluminum oxide to a carbon- and PTFE-containing layer. Inside the pores and caverns, the coating contains agglomerates of dispersed PTFE particles, as shown in Fig. 6. According to elemental analysis of the cross section, the concentration of fluorine and, accordingly, PTFE increases toward the coating/air boundary, shown in Figs. 4c and 5b.

According to previously performed measurements using X-ray photoelectron spectroscopy [24], the coating surface (composition of a layer thickness approximately 3 nm was analyzed) formed in a base electrolyte + 100 mL/L emulsion + 60 g/L PTFE particles contains approximately 9% CF_2 groups (of the total carbon content), 10.8% CO_2 , and 14.6% CO.

The main mass (65.5%) of the surface coating layer consists of aliphatic carbon (CC or CH bonds). Traces of PTFE decomposition have been observed in the form of CF groups.

Adhesion of Coatings to the Aluminum Substrate

As follows from the previous material, the composition of coatings differs strongly from the oxide composition of traditional PEO coatings on valve metals. Coatings produced in an electrolyte suspension consist of carbon compounds and PTFE. Nevertheless, coatings possess an adequate adherence to aluminum alloy. They do not separate from the substrate during sample deformation and after extensive pressure from a moving cutting-steel tip during wear investigation [23]. This is supported by results of adhesion to substrate investigations by means of ultrasound, as shown in Fig. 7. The application of this method, which has been described in detail in the literature for adhesion investigation of oxide coatings to metals [27, 28], yields a postultrasound mass loss result of 1.5–2.0% (100 W over 10 min). In our case, the sample mass change does not exceed 1% after 20 min of treatment, which is evidence of a relatively strong adhesion to the substrate and a strong cohesion of a coating fragment. The external appearance of coatings practically does not change, and neither does the thickness. If we consider that, during ultrasonic treatment, only certain fragments of the coating break off, then, according to the data and results of weighing of samples both prior to PEO and of those with coatings formed in electrolytes of type base + emulsion + PTFE, the weight loss after ultrasonic treatments is 5–29%. Thus, coatings have a relatively strong cohesion between fragments.

Corrosion Resistance Characteristics of Coatings

The protective characteristics of coatings were evaluated on the basis of measurement of pitting formation time in the coatings as a result of contact with a 3% NaCl drop during initiation of the process by a potential difference from 1 to 8 V between the drop and the metallic substrate, as shown in Table 2. Data acquired from various applied potentials correlate. Table 2 shows that the protective characteristics of light regions is greater than those of dark regions. This corresponds with the notably lower porosity of light regions compared to that of dark regions, as can be seen in Fig. 3, and they contain more PTFE, as can be seen in table 1. On the other hand, the data in Table 2 suggest that the pitting formation time depends on the exposure time of the sample to air. It stabilizes by the fourth day of exposure. The distribution of data based on pitting formation time for samples kept in air for greater than 4 days is likely related to the solution test drop coming into contact randomly with both dense regions and with the large gaps in the surface, seen in Fig. 3. Annealing the sample at 100°C for 1 h prior to

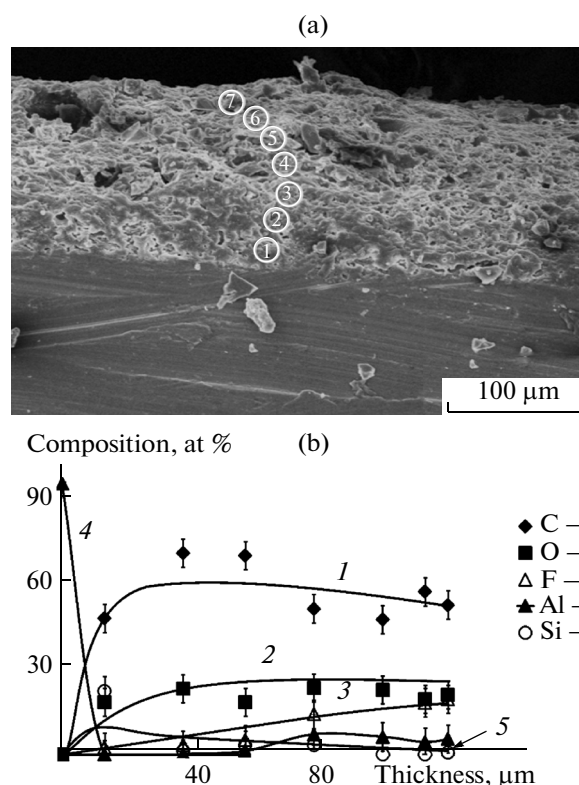


Fig. 5. (a) SEM image of coating cross section on aluminum and (b) distribution of majority elements across the coating cross section.

treatment produces an analogous effect. It is therefore likely that increased pitting formation time is related in both cases with a certain “drying” of surfaces and coating densification. The coating possesses generally poor protective characteristics as a result of inadequate corrosion resistance of the dark regions.

Table 2 shows that coating annealing at 100°C significantly increases pitting formation time for both light and dark regions in coatings kept in air for 4 or more days. It appears that the effect is connected not only to evaporation but, as has been observed in existing works, also with the sealing effect of PTFE particles flowing and densifying in coating pores [12, 16]. This conclusion is experimentally confirmed below.

Table 3 shows that the introduction of emulsion and, subsequently, of PTFE particles into the base electrolyte improves the protective properties of light regions in the coating. The greater the powder concentration, i.e., the greater the coating thickness, the greater the pitting formation time. Coating thickness with increased PTFE powder concentration increases from ~10 to ~80 μm [23]. The relation of pitting formation time to coating thickness; i.e. the calculation of the t/h value, as shown in table 3, shows that the thickest coatings are formed at PTFE concentrations of 20–30 g/L.

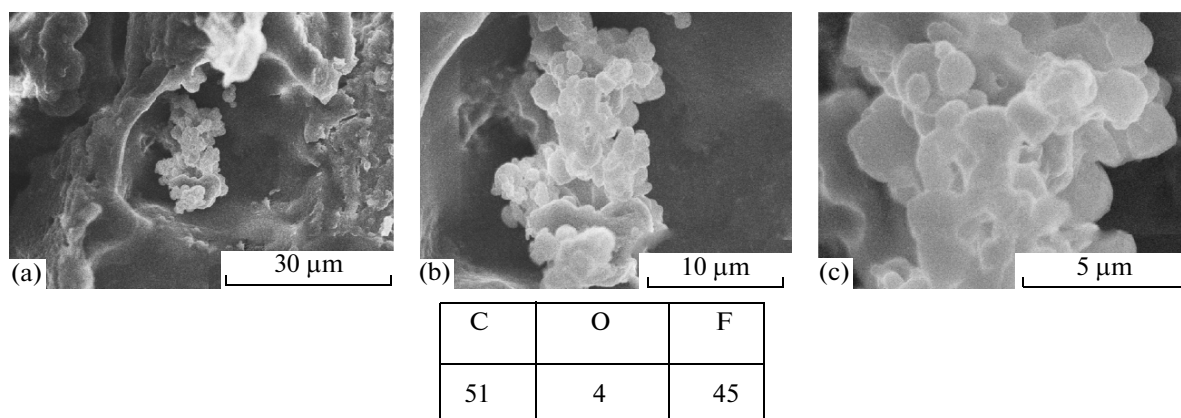


Fig. 6. (a) Cavern in the coating core (a) and (b, c) dispersed particles sealed in the cavern; elemental composition (at %) of dispersed particles in cavern determined using an energy-dispersive module for a scanning electron microscope.

We note that, as concentration of PTFE powder in the electrolyte increases, the protective characteristics of the dark regions increase as well, likely due to their increased PTFE content and due to pore sealing by PTFE particles. The presence of PTFE particles in coating pores at high concentrations of PTFE in the electrolyte suspension—emulsion is shown both in this work and can be found in the literature [23].

Change of Morphology; Thickness; Composition; and Hydrophobic, Hydrophilic, and Protective Characteristics of Coatings after Heat Treatment

Figure 8 shows the change in surface morphology of coatings after 2-h annealing in air at 100, 200, 300 and 400°C. Images were acquired using a laser confocal microscope on randomly selected regions of the coating surface. Craters with a diameter up to 150 μm

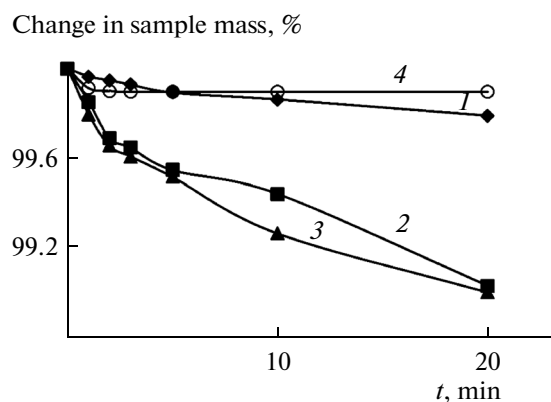


Fig. 7. Change in sample mass under ultrasound. Coatings are formed (1) in base electrolyte, (2) in base electrolyte + 100 mL/L emulsion, (3) in base electrolyte + 100 mL/L emulsion + 20 g/L PTFE powder, and (4) in base electrolyte + 100 mL/L emulsion + 40 g/L PTFE powder.

can be seen on the surface of initial (Fig. 8a) coatings and coatings that have been annealed at 100°C (Fig. 8b) that have been filled with molten material along with chaotically distributed deep pits—likely pores—several tens of microns in diameter. Figure 8c shows that, after annealing at 200°C, almost all craters and pores are filled and sealed. After annealing at 300°C (Fig. 8d), there are no observable craters or pores on the surface. After annealing at 400°C (Fig. 8e), the surface appears smooth, with scattered protruding “islands.”

The thickness (Fig. 9a), roughness (Fig. 9b), wetting contact angle (Fig. 9c), and elemental composition (Fig. 10) of the surface of PTFE-oxide coatings behave in the same manner.

The thickness of the initial coating formed in the base electrolyte (Fig. 9a, curve 1) remains within the margin of error of the measurements of the constant. Its tendency to increase is observed at temperatures above 400°C. This is related to oxygen starting to penetrate through pores and cracks to the surface, leading to thermal oxidation [31]. The thicknesses of PTFE-oxide coatings are temperature-resistant to 100–200°C. At higher temperatures, the thickness drops quickly, reaching values characteristic of coatings formed in the base electrolyte, i.e., ~10–15 μm. The surface roughness of PTFE-oxide coatings starts to reduce in an analogous fashion above temperatures of 100–200°C, reaching values characteristic of the initial coating (Fig. 9b). The wetting contact angle increases as annealing temperature increases, reaching maximum values for coatings annealed at 300°C (Fig. 9c). This occurs at temperatures where no pores and craters are present on the surface and the polymer coating noticeably sublimates (Fig. 8d). At annealing temperatures of 400°C, its value corresponds with that of the initial coating.

The elemental composition of coatings analyzed to a depth of 2–5 μm by means of microprobe X-ray spectroscopy and shown in Fig. 10 changes in a similar

Table 2. Influence of sample surface structure and air exposure on pitting formation time during process initiation by potential differences of 1 and 8 V. Coatings are formed in electrolyte of composition 10.6 g/L Na₂SiO₃ + 2 g/L NaOH + 100 mL/L siloxane emulsion + 10 g/L PTFE over 20 min

Sample operations		Pit formation time, s			
		light region		dark region	
Air exposure, days	Air exposure at 100°C, 1 h	<i>U</i> = 1 V	<i>U</i> = 8 V	<i>U</i> = 1 V	<i>U</i> = 8 V
0*	—	38 ± 5	8 ± 1	~1	~1
1	—	135 ± 37	40 ± 9	~1	~1
4	—	300 ± 90	54 ± 12	~1	~1
5	—	189 ± 32	56 ± 13	~1	~1
7	—	243 ± 70	66 ± 6	~1	~1
—	Yes**	501 ± 84	344 ± 45	325 ± 72	35 ± 18

* Approximately after half an hour after coating formation; **approximately 10 min after annealing of freshly produced sample with coating

Table 3. Pitting formation time for surfaces formed in base electrolyte of 10.6 g/L Na₂SiO₃ + 2 g/L NaOH with addition of 100 mL/L siloxane acrylate emulsion into base electrolyte and, subsequently, various amounts of PTFE powder. Coatings are formed over 20 min

Electrolyte	coating test	Pitting formation time <i>t</i> , s					
		light region				dark region	
		<i>U</i> = 1 V	<i>t/h</i> , s/μm	<i>U</i> = 8 V	<i>t/h</i> , s/μm	<i>U</i> = 1 V	<i>U</i> = 8 V
Base	A	—	—	—	—	~1	~1
	B	—	—	—	—	~1	~1
+ emulsion	A	70	7	11	1.1	—	—
	B	253	25.3	49	4.9	—	—
+10 g/L	A	38	3.8	8	0.8	~1	~1
	B	300	30.0	54	5.4	~1	~1
+20 g/L	A	138	10.6	60	4.6	7	~1
	B	453	34.8	80	6.2	105	~1
+30 g/L	A	270	12.3	87	4.0	1	~1
	B	423	19.2	209	9.5	200	162
+40 g/L	A	50	1.3	3	0.1	~1	~1
	B	721	18.0	144	3.6	~1	~1
+50 g/L	A	72	1.1	32	0.5	132	18
	B	953	14.7	274	4.2	312	36

(A) After approximately half an hour after coating formation; (B) after air exposure for 5 days. Pitting formation time is presented for a potential difference of 1–8 V. *t/h*, s/μm is pitting formation time related to coating unit thickness. Coating thickness data are taken from the literature [23].

fashion. The amount of carbon, aluminum, and oxygen present in coatings is stable up to 200°C and subsequently changes, reaching values characteristic of the initial coating acquired in the base electrolyte.

From data on the temperature-related behavior of surface morphology, its thickness, roughness, hydrophilic–hydrophobic balance, and elemental composition of PTFE–oxide coatings, we can conclude that, up to temperatures of 100–200°C, their parameters are stable. At higher annealing temperatures, the polymer coating starts to flow, eventually spreading over the surface. This is clearly illustrated in Fig. 8c, where pores and craters are filled with polymer. After annealing at 300°C, they are not visible on the surface. How-

ever, at temperatures above 200°C, alongside partial flow, a sublimation of the polymer and carbon-containing part of the coating is observed. This is also evident in data on the thickness and roughness reduction of coatings (Figs. 9a, 9b) and the nature of the change of majority elemental composition of coatings—specifically, carbon and fluorine (Fig. 10). According to all the investigated characteristics at annealing temperatures of 400°C, the polymer and carbon-containing part of the coating sublimates, leaving the substrate coating of thickness approximately 10–15 μm with parameters characteristic of a coating formed in the base electrolyte.

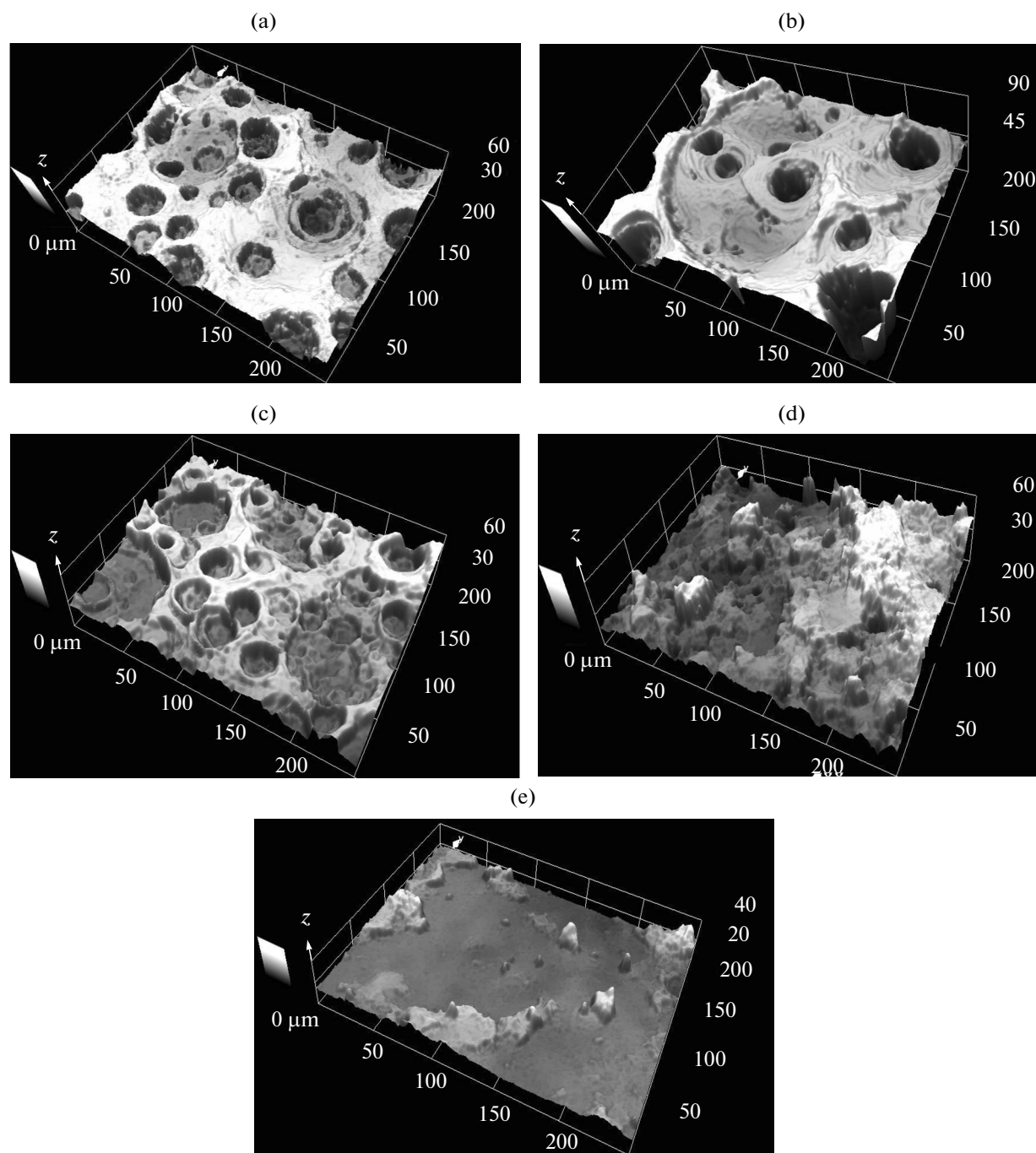


Fig. 8. Influence of heat on surface morphology of PTFE-oxide coatings. Annealing temperature in air, °C: (a) initial coating, (b) 100, (c) 200, (d) 300, and (e) 400. Coatings are formed in base electrolyte + 100 mL/L emulsion + 40 g/L PTFE powder.

The established facts on the influence of temperature on the investigated characteristics of PTFE-oxide coatings correlate well with the tendencies established for composite coatings with a tribologically applied layer of dispersed PTFE particles onto a PEO coating [12, 16]. In these investigations, it was established that, depending on the fraction, at temperatures of

100–250°C the powder softens and acquires the ability to flow, which results in pore and crack sealing and improvement of the coating's corrosion resistance.

In the investigated PTFE-oxide coatings, the sealing of pores and craters as a result of the coating's polymer part starting to flow leads to improvement of the coating's corrosion resistance, as shown in Fig. 11.

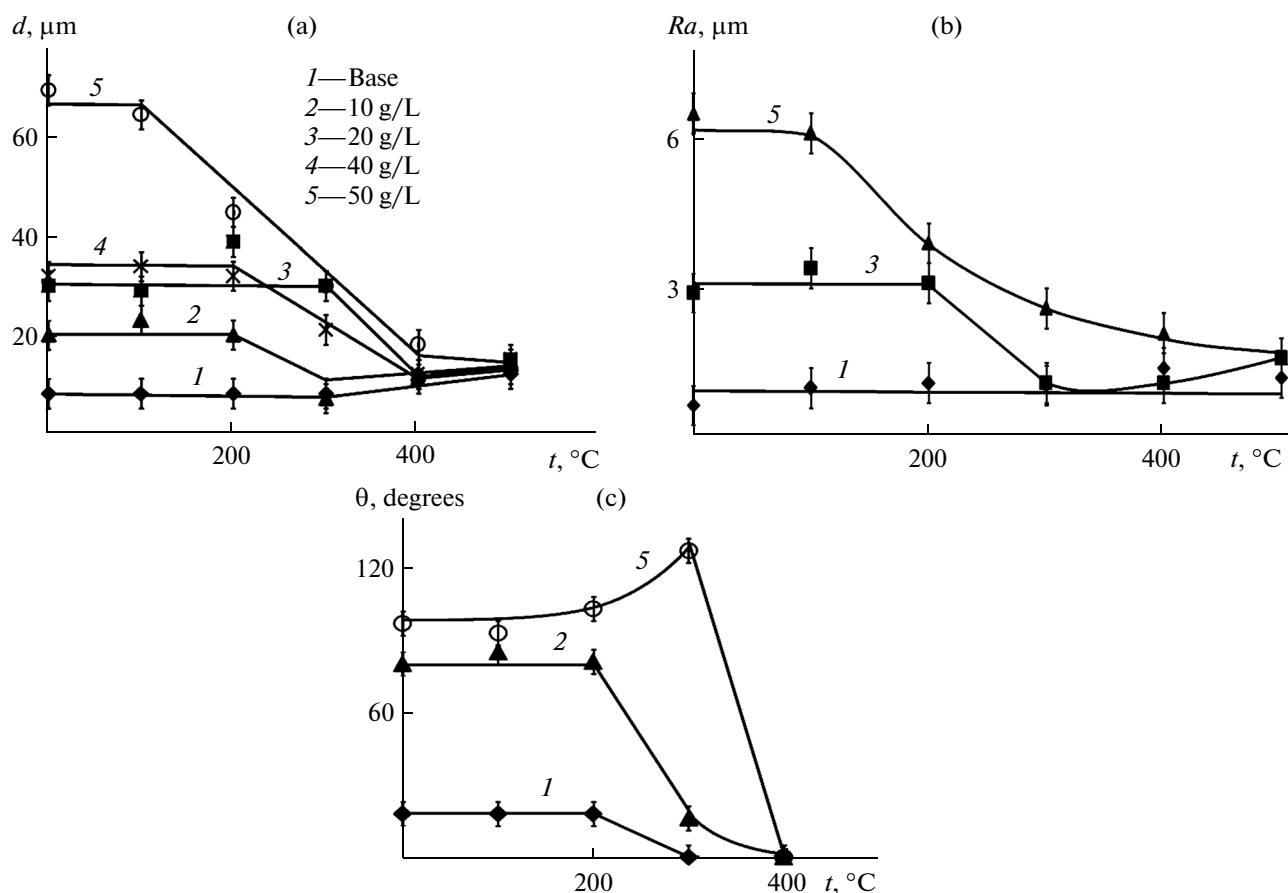


Fig. 9. Influence of heat on (a) thickness and (b) surface roughness Ra of PTFE oxide coatings; (c) wetting contact angle for dark surface regions. Coatings are formed in electrolyte: (1) base ($\text{Na}_2\text{SiO}_3 + \text{NaOH}$); (2–5) base + emulsion + X g/L PTFE particles. X = 2–10, 3–20, 4–40, and 5–50.

Similar tendencies to those in Fig. 11 were established in the system in which pitting formation was initiated by a potential difference of 8 V across a solution/metal boundary. The best protective properties were possessed by coatings annealed at 200 $^{\circ}\text{C}$, i.e., when the thickness, composition, and other coating parameters have not yet begun to significantly change but the flowing polymer has filled cracks and pores (Fig. 8c).

DISCUSSION

In earlier works, we have presented a method for the use of suspension–emulsion electrolytes using a siloxane acrylate emulsion that allows for the production of stable hydrous electrolytes with dispersed PTFE or graphite particles that do not phase separate over at least a month [22–25]. Coatings formed using PEO in suspension–emulsion electrolytes with PTFE particles on aluminum alloy fundamentally differ in structure from traditional oxide coatings. If the latter are composed primarily of metal oxides, then the coatings that we have produced have a layered structure. In the region of metallic contact, a coating exists that is similar in composition and thickness to an oxide coat-

ing formed in a base electrolyte—in our case, $\text{Na}_2\text{SiO}_3 + \text{NaOH}$. Above it is a layer containing mostly carbon, oxygen, and fluorine, as shown in Figs. 4 and 5. During PEO, the dispersed PTFE powder transforms into a compact, dense state, likely due to sintering and partial polymerization. Agglomerates of dispersed PTFE powders remain in pores and caverns, both open to the surface and in the depth of the layer.

The exterior surface of the carbon-containing layer, under selected production conditions, consists of regions of different coloring: light and dark. These regions differ in morphology, corrosion resistance, and composition. As dark regions have a surface that has more defects, pores, and caverns, they are characterized by inadequate corrosion resistance. As a result, initial coatings in general have poor protective properties in chlorine-containing environments. As dark regions are formed on the surface of light regions and contain large caverns and pores, it can be concluded that they are formed under the influence of arc discharges on light regions. The established facts allow us to conclude that, at a lower coating formation time or lower current density, coatings can be produced that consist of only light regions with improved corrosion

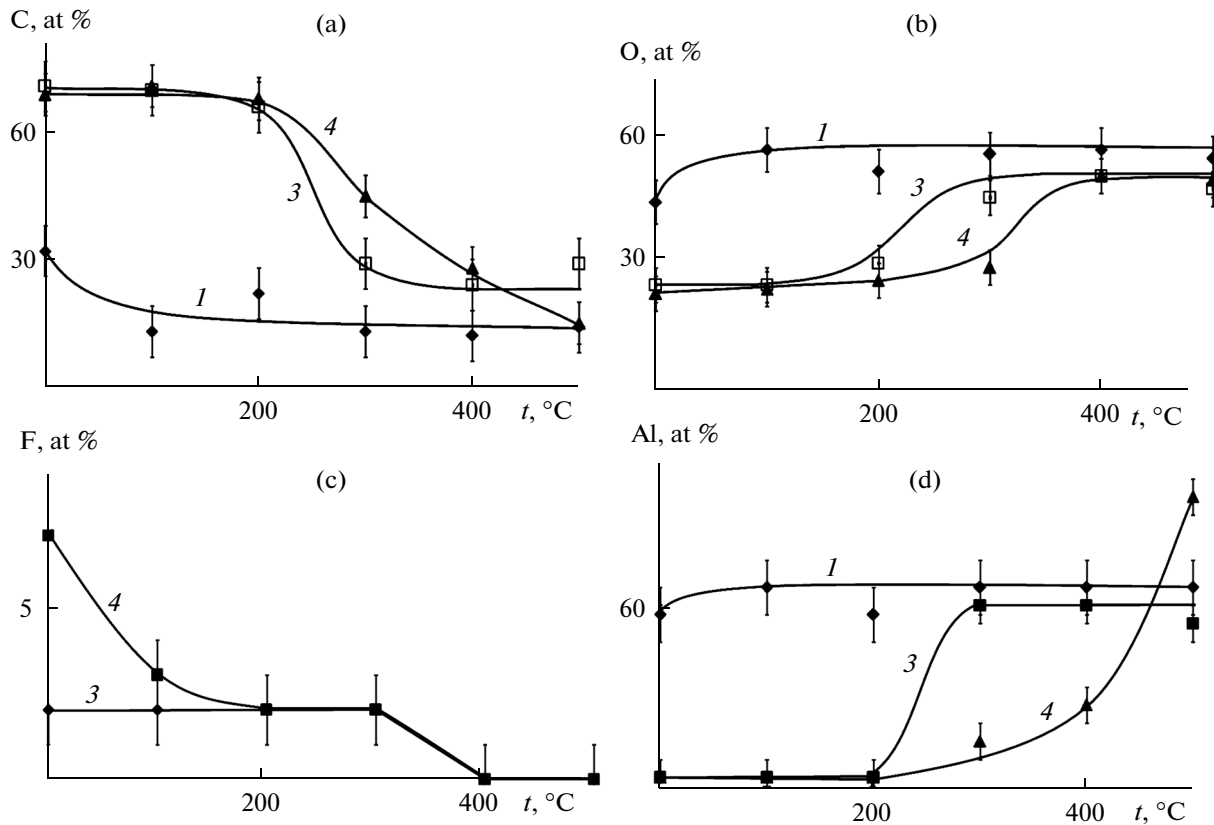


Fig. 10. Change of coating elemental composition after annealing. (a) Change of carbon content, (b) change of oxygen content, (c) change of fluorine content, and (d) change of aluminum content. Curves marked as in Fig. 9.

resistance characteristics. From these points of view, it becomes useful to study the tendencies of the formation of PTFE-oxide coatings and with different current forms—for example, a bipolar anodic-cathodic current with varying pulse frequency. Subsequent investigations will study these.

PTFE-oxide coatings formed using PEO formed in one stage in the studied electrolytes are similar in certain characteristics to PTFE applied to the metal and provide significant wear time under stress and hydrophobicity [23]. With these properties taken into consideration, the acquired coatings and their method of production can be recommended for practical use.

It follows from the obtained results that protective characteristics and coating surface morphology can be significantly altered by annealing at 200°C. The reason for this is that PTFE particles start to flow and fill pores. This behavior corresponds with the behavior of composite coatings produced by a combination of PEO and subsequent tribological application of PTFE [12, 16].

According to the obtained data on elemental and phase composition, produced layers contain PTFE. In all likelihood, the main volume of the coating consists of PTFE and products of its partial sublimation and decomposition, as well as the products of sublimation

and decomposition of the siloxane acrylate emulsion. As flow is observed at 200°C and significant sublimation of the carbon- and fluorine-containing layer is observed above 300°C, it seems to be primarily composed of polymers. The heat-related properties of carbon- and fluorine-containing layers correspond with the literature data for Forum dispersed PTFE. According to chromatographic analysis, Forum contains components with a carbon number ranging from C_5 to C_{70} , among them saturated and unsaturated fluorocarbons [30]. We note that sublimation, not pyrolysis, is characteristic for fractions of dispersed Forum PTFE “Forum” [32]. The following sublimation fractions have been selected from among the components of dispersed Forum PTFE: up to 70°C, 70–100, 100–150, 150–200, up to 220, and up to 310°C [30]. Light PTFE from C_4 to C_{12} are present in the sublimation fraction of 70–200°C, and from 220°C the most intense sublimation component is C_{16} fluorocarbon. Fractions with a sublimation temperature of up to 310°C are a number of heavy fluorocarbons [30]. It seems that the sublimation characteristics also determine the heat-dependent properties of the condensed coating. As the amount of carbon detected in the depth of the coating and on its surface is significantly greater than that of fluorine, it is possible that, in addition to PTFE, the layer contains other polymers

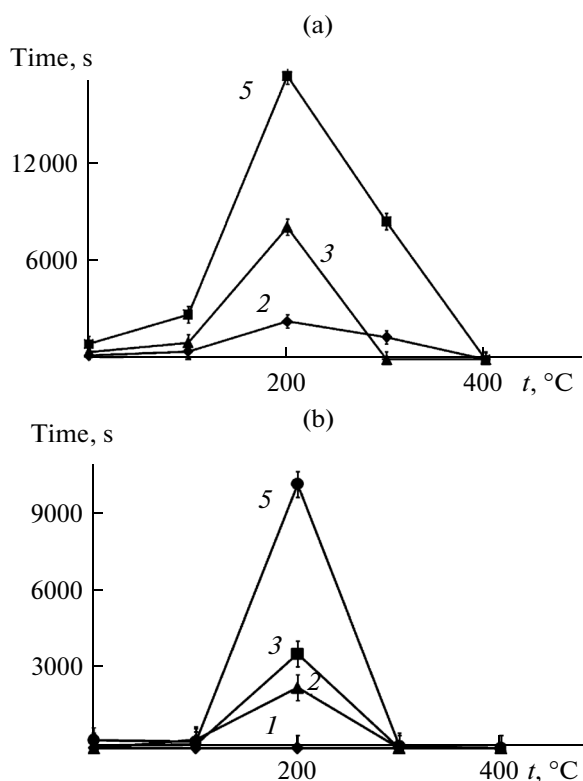


Fig. 11. Influence of annealing temperature on pitting formation time initiated by applied potential difference of 1 V. (a) For light coating regions and (b) for dark coating regions. Curves marked as in Fig. 9.

formed under the influence of electrical discharges during PEO.

As a result of sublimation of the exterior carbon- and fluorine-containing layer, the investigated coatings function only up to temperatures of $\sim 250^{\circ}\text{C}$. However, heating up to these temperatures improves the tribological and protective properties.

We note that the presented approach permits stabilization of electrolytes using not only PTFE, but also graphite, and, it seems, other dispersed particles of organic or inorganic nature, introducing them during PEO in such electrolytes into the coating.

CONCLUSIONS

1. It has been illustrated that coatings formed in suspension-emulsion electrolytes with dispersed PTFE particles in a siloxane acrylate emulsion by means of a single-stage PEO process on aluminum alloy have a layered structure. The layer adjacent to the metal transitions from Al_2O_3 to polymer. The thickness of the polymer layer depends both on the formation conditions and the concentration of PTFE particles in the electrolyte.

2. Coatings have been produced the surface of which consists of regions that differ in composition,

thickness, and the presence and size of pores and caverns and pitting formation resistance in chlorine-containing environments.

3. It has been established that, during annealing in air at 200°C , the polymers that form the outer part of the coating start to flow and fill pores and caverns, which greatly improves the protective properties of coatings.

4. During annealing in air at 400°C , the entire polymer part of the coating sublimates. However, a thin oxide layer remains with parameters characteristic for a layer formed in the base electrolyte (no emulsion or PTFE particles).

REFERENCES

1. Mu, M., Zhou, Xj., and Xiao, Q., *Appl. Surf. Sci.*, 2012, vol. 258, no. 22, pp. 8570–8576.
2. Wu, Xh., Qin, W., Guo, Y., and Xie, Zy., *Appl. Surf. Sci.*, 2008, vol. 254, no. 20, pp. 6395–6399.
3. Martini, C., Ceschini, L., Tarterini, F., et al., *Wear*, 2010, vol. 269, nos 11–12, pp. 747–756.
4. Fuks, S.L., Devyaterikova, S.V., and Khitrin, S.V., *Rus. J. Appl. Chem.*, 2013, vol. 86, no. 6, pp. 848–852.
5. Mandelli, A., Bestetti, M., Da, Forno A., et al., *Surf. Coating. Techn.*, 2011, vol. 205, no. 19, pp. 4459–4465.
6. Blawert, C., Sah, S.P., Liang, J., et al., *Surf. Coat. Technol.*, 2012, vol. 213, pp. 48–58.
7. Lamaka, S.V., Knoernschild, G., Snihirova, D.V., et al., *Electrochem. Acta*, 2009, vol. 55, no. 1, pp. 131–141.
8. Lee, K.M., Ko, Y.G., and Shin, D.H., *Curr. Appl. Phys.*, 2011, vol. 11, no. 4, pp. S55–S59.
9. Lv, G.H., Chen, H., Gu, W.C., et al., *Curr. Appl. Phys.*, 2009, vol. 9, no. 2, pp. 324–328.
10. Bryuzgin, E.V., Takahashi, K., Navrotsky, A.V., et al., *Prot. Met. Phys. Chem. Surf.*, 2012, vol. 48, no. 2, pp. 184–190.
11. Xu, Q., Yang, Y., Wang, X., et al., *J. Membr. Sci.*, 2012, vol. 415, pp. 435–443.
12. Gnedenkov, S.V., Sinebryukhov, S.L., Mashtalyar, D.V., et al., *Prot. Met.*, 2008, vol. 44, no. 7, pp. 704–709.
13. Drelich, J., Chibowski, E., Meng, D.D., and Terpilowski, K., *Soft Matter*, 2011, vol. 7, no. 21, pp. 9804–9828.
14. Suminov I.V., Epelfeld A.V., Lyudin V.B., Krit B.L., Borisov A.M. Microarc oxidation (theory, technology, equipment). M.:EKOMET, 2005. 368 s.
15. Rakoch, A.G., Dub, A.V., and Gladkova, A.A., *Anodization of light alloys at varying electrical regimes. Plasma-electrolytical nanotechnology*, Moscow: Izd-vo "Staraya Basmanaya", 2012. 496 s.
16. Gnedenkov, S.V., Sinebryukhov, S.L., and Sergienko, V.I., *Composite multifunctional coatings formed on the metals and alloys by plasma electrolytic oxidation*, Vladivostok: Dalnauka, 2013. 460 p.
17. Gruss, L.L. and McNeil, W., *Electrochem. Technol.*, 1963, vol. 1, nos 9–10, pp. 283–287.
18. Saakiyan, L.S., Efremov, A.P., Epel'fel'd, A.V., et al., *Fiz.-Khim. Mekh. Mater.*, 1987, no. 6, pp. 88–90.

19. Wang, Y., Jiang, Z., Liu, X., and Yao, Z., *Applied Surface Science*, 2009, vol. 255, pp. 8836–8840.
20. Karpushenkov, S.A., Kulak, A.I., Shchukin, G.L., and Belanovich, A.L., *Prot. Met. Phys. Chem. Surf.*, 2010, vol. 46, no. 4, pp. 463–468.
21. Karpushenkov, S.A., Shchukin, G.L., Belanovich, A.L., et al., *J. Appl. Electrochem.*, 2010, vol. 40, pp. 365–374.
22. Rudnev, V.S., Vaganov-Vil'kins, A.A., Nedorozov, P.M., et al., *Rus. J. Appl. Chem.*, 2012, vol. 85, no. 8, pp. 1147–1152.
23. Rudnev, V.S., Vaganov-Vil'kins, A.A., Nedorozov, P.M., et al., *Prot. Met. Phys. Chem. Surf.*, 2013, vol. 49, no. 1, pp. 87–94.
24. Rudnev, V.S., Ustinov, A. Yu., Vaganov-Vil'kins, A. A., et al., *Rus. J. Phys. Chem. A*, 2013, vol. 87, no. 6, pp. 1021–1026.
25. Patent RF 2483144, Method for obtaining composite polymer-oxide coatings on valve metals and alloys / Rudnev V.S., Vaganov-Vil'kins A.A., Yarovaya T.P., Nedorozov P.M., published 27.05.2013, Bull. no. 15.
26. Wang, W., Lin, C., and Tang, Z.G., *J. Technol. (National Taiwan Univer. Sci. Techn.)*, 2010, vol. 10, pp. 65–67.
27. Banus, E.D. Ulla, M.A., et al., *Appl. Catal. A-Gen.*, 2011, vol. 393, pp. 9–16.
28. Cebollada, P.A.R. and Bordeje, E.G., *Chem. Eng. J.*, 2009, vol. 149, pp. 447–454.
29. Gordienko, P.S. and Rudnev, V.S., *Electrochemical formation of coatings on aluminium and its alloys at spark and breakdown potentials*, Vladivostok: Dal'nauka, 1999.
30. Pavlov, A.D., Sukhoverkhov, S.V., and Tsvetnikov, A.K., *Vestnik DVO RAN*, 2011, no. 5, pp. 72–75.
31. Lysenko, A.E., Rudnev, V.S., and Vaganov-Vil'kins, A.A., *Korroziya: Materialy, zashchita*, 2008, no. 3, pp. 25–29.
32. Pavlov, A.D., Sukhoverkhov, S.V., and Tsvetnikov, A.K., *Vestnik DVO RAN*, 2013, no. 5, pp. 39–43.

Translated by S. Punzhin